Crystal Structure of a Four-Copper Laccase Complexed with an Arylamine: Insights into Substrate Recognition and Correlation with Kinetics † , ‡

ARTICLE *in* BIOCHEMISTRY · JULY 2002

Impact Factor: 3.02 · DOI: 10.1021/bi0201318 · Source: PubMed

7 AUTHORS, INCLUDING:

Thomas Bertrand
Sanofi Aventis Group
22 PUBLICATIONS **689** CITATIONS
SEE PROFILE

Claude Jolivalt
MINES ParisTech
66 PUBLICATIONS **1,259** CITATIONS
SEE PROFILE

Catherine Madzak
French National Institute for Agricultural Res…
66 PUBLICATIONS **1,778** CITATIONS
SEE PROFILE

Christian Mougin
French National Institute for Agricultural Res…
117 PUBLICATIONS **1,541** CITATIONS
SEE PROFILE

Crystal Structure of a Four-Copper Laccase Complexed with an Arylamine: Insights into Substrate Recognition and Correlation with Kinetics[†,‡]

Thomas Bertrand,[#] Claude Jolivalt,[§] Pierre Briozzo,*[,||,#] Eliane Caminade,[§] Nathalie Joly,[||] Catherine Madzak,[⊥] and Christian Mougin[§]

Laboratoire d'Enzymologie et Biochimie Structurales, UPR 9063 du CNRS, 91198 Gif-sur-Yvette Cedex, France, Laboratoire de Phytopharmacie et Médiateurs Chimiques, INRA, route de Saint-Cyr, 78026 Versailles Cedex, France, Laboratoire de Chimie Biologique, Institut National Agronomique Paris-Grignon, 78850 Thiverval-Grignon, France, Laboratoire de Génétique Moléculaire et Cellulaire, INRA, 78850 Thiverval-Grignon, France

Received February 13, 2002; Revised Manuscript Received April 1, 2002

ABSTRACT: Laccases are multicopper oxidases that catalyze the oxidation of a wide range of phenols or arylamines, and their use in industrial oxidative processes is increasing. We purified from the white rot fungus *Trametes versicolor* a laccase that exists as five different isozymes, depending on glycosylation. The 2.4 Å resolution structure of the most abundant isozyme of the glycosylated enzyme was solved. The four copper atoms are present, and it is the first crystal structure of a laccase in its active form. The crystallized enzyme binds 2,5-xylidine, which was used as a laccase inducer in the fungus culture. This arylamine is a very weak reducing substrate of the enzyme. The cavity enclosing 2,5-xylidine is rather wide, allowing the accommodation of substrates of various sizes. Several amino acid residues make hydrophobic interactions with the aromatic ring of the ligand. In addition, two charged or polar residues interact with its amino group. The first one is an histidine that also coordinates the copper that functions as the primary electron acceptor. The second is an aspartate conserved among fungal laccases. The purified enzyme can oxidize various hydroxylated compounds of the phenylurea family of herbicides that we synthesized. These phenolic substrates have better affinities at pH 5 than at pH 3, which could be related to the 2,5-xylidine binding by the aspartate. This is the first high-resolution structure of a multicopper oxidase complexed to a reducing substrate. It provides a model for engineering laccases that are either more efficient or with a wider substrate specificity.

Multicopper oxidases combine the four-electron reduction of dioxygen to water with the one-electron oxidation of four reducing substrate molecules. The well-defined members of this class are laccase, ascorbate oxidase, and ceruloplasmin (for a review, see refs *1* and *2*). Laccases (*para*-diphenol: dioxygen oxidoreductases, EC 1.10.3.2) are generally glycosylated. Most are extracellular enzymes, and a given species may produce isozymes of both extra- and intracellular types. They are produced by various fungi, plants, and certain bacteria or insects. It has been proposed that plant laccases—in particular tree enzymes—catalyze during lignification the initial polymerization of monolignols by oxidatively coupling them into dimers and trimers. Then, peroxidases synthesize the extended polymeric lignins from oligolignols (*1*). In contrast, fungal laccases play a role in lignin degradation. Their in vivo functions also include fungal virulence, pigment formation, and detoxification of phenols produced during lignin degradation (*3*).

Laccases contain four copper ions distributed into three sites, defined according to spectroscopic properties. The T1 site contains the type 1 blue copper (Cu1), whose tight coordination to a cysteine is responsible for an intense absorption band around 600 nm, giving its blue color to the enzyme. The T2 site contains a type 2 copper (Cu2) with a characteristic electron paramagnetic resonance (EPR). In the T3 site, the pair of strongly coupled type 3 coppers (Cu3a and Cu3b) is EPR-silent in the presence of dioxygen, indicative of a strongly antiferromagnetically coupled Cu pair bridged by a hydroxide. The mononuclear T1 site extracts electrons from the reducing substrate and mediates their transfer to the trinuclear T2/T3 center where molecular oxygen is reduced.

Laccases' substrates are mostly phenols or arylamines. As these enzymes have a low substrate specificity, they can oxidize a variety of substrates, either of natural or industrial origin. Fungal laccases are marketed for bleaching in the textile and dye industry. Other potential applications include the paper industry, enzymatic conversion of chemical intermediates, or oxidative transformation of environmental pollutants. Among the herbicides used for weed control, phenylurea derivatives have been extensively spread in the environment since their discovery in the 1950s. They are used both on cultivated (selective germination of cereal crops) and uncultivated (maintenance of roads, railways) areas. There is a growing concern over the potential of

[†] This work was supported by grants from the Centre National de la Recherche Scientifique (UPR 9063), and the Institut National de la Recherche Agronomique (UR 258 and UMR 206).

[‡] Atomic coordinates: pdb accession number 1KYA.

* Corresponding author. E-mail: briozzo@grignon.inra.fr.

[#] Laboratoire d'Enzymologie et Biochimie Structurales, UPR 9063 du CNRS.

[§] Laboratoire de Phytopharmacie et Médiateurs Chimiques, INRA.

[||] Institut National Agronomique Paris-Grignon.

[⊥] Laboratoire de Génétique Moléculaire et Cellulaire, INRA.

10.1021/bi0201318 CCC: $22.00
Published on Web 05/14/2002

herbicides to contaminate soils, and surface or groundwater. Among them, the chlorinated aromatic compounds tend to accumulate because of their low solubility in water. Moreover, several chlorophenols are carcinogenic. However, microorganisms can degrade them in soils. One possible initial step in this transformation pathway proceeds via the hydroxylation of the aromatic ring. This was reported in the case of the herbicide metoxuron (*4*), and also for the metabolization of diuron (*5*) and monuron (*6*) by plants. In soils, photolysis of phenylurea herbicides exposed to sunlight can lead to ring hydroxylation for monuron (*7*), and in particular to the 2- and 4-hydroxylation of the aromatic ring for fenuron (*8*). Such a functionalization of the aromatic ring considerably extends the possible metabolic pathways. However, chlorinated hydroxyphenylurea herbicides are very difficult to degrade by aerobic microorganisms: these compounds are acutely toxic, as they uncouple oxidative phosphorylation.

White rot fungi are good candidates for further degradation of phenylureas in soil because they elude this toxicity problem. As most of their oxidative enzymatic systems involved in the transformation are extracellular, compounds do not need to be internalized prior to the degradation. These fungi can degrade a wide range of chlorinated phenols (*9*). In particular, laccases of *Trametes versicolor* have been reported to be involved in this process (*10*). We recently sequenced (accession number AF414109), purified, and crystallized a laccase secreted by *T. versicolor* (*11*). Several sequences of laccases have been deposited for this basidiomycete. As the enzyme we studied shares 99.2% sequence identity—only four residues are different—with the laccase III from *T. versicolor* (sequence accession number D13372; (*12*)), we name it laccase IIIb (LacIIIb).[1] Starting from such laccases, it would be of interest to design enzymes that are either more efficient in catalysis or are capable of oxidizing a wider variety of reducing substrates.

However, there are not enough detailed structural data to allow such engineering, or even to understand laccase specificity and oxidation mechanism. The only known crystal structure of a laccase is that of the fungus *Coprinus cinereus* (Lac-Cc). In the two published models calculated either with data collected at room temperature (pdb code 1A65; (*13*)) or at 100 K (1HFU; (*14*)), the crystallized enzyme was trapped in a form devoid of the type 2 copper. This depletion completely inactivates laccases (*15*). Here we present the crystal structure of the active LacIIIb, allowing description of the trinuclear T2/T3 site. Furthermore, in all known high-resolution structures of multicopper oxidases (ascorbate oxidase from Zucchini (*16*) and Lac-Cc) the putative cavity for the reducing substrate is empty. For the multifunctional human enzyme ceruloplasmin, structures that locate the binding site for complexed biogenic amines, in a cavity close to the mononuclear type I blue copper site, have been published, but their resolution is limited to 3.1 Å or less, so that the authors did not refine this binding site (*17*). The structure presented here contains an arylamine, likely the laccase production inducer 2,5-xylidine (2,5-dimethylbenzenamine). This pinpoints key residues important for substrate binding.

As indicated above, the degradation of hydroxyphenylurea compounds by fungal laccases is of environmental interest. For this reason, and also to obtain additional information on enzyme/substrate interaction, we synthesized a series of isomers of such compounds. They differ by the respective positions of urea and hydroxyl substituents, and by the eventual presence of a chlorine substituent, on the aromatic ring. The kinetic parameters obtained for these derivatives are discussed in relation with the crystal structure.

EXPERIMENTAL PROCEDURES

Chemicals. Solvents used for high performance liquid chromatography (HPLC) analysis were purchased from Carlo Erba. 2,5-xylidine, ABTS [2,2′-azino-bis(3-ethylbenzthiazoline-6-sulfonic acid)], and all chemicals and reagents used for the synthesis of hydroxyphenylurea compounds were purchased from Sigma-Aldrich, Acros, and Lancaster.

Production of the Purified Enzyme. The production and purification of LacIIIb have been described elsewhere (*11*). Briefly, the enzyme was produced from *T. versicolor* cultures induced by 2,5-xylidine. The purification included two steps of chromatography: first on a DEAE 52 anion exchange column, and then on a hydrophobic interaction Phenyl sepharose column. This latter chromatography further improved the enzyme purity, as checked by sodium dodecyl sulfate—polyacrylamide gel electrophoresis, which gave a unique band.

Isoelectric Focusing. Isoelectric focusing (IEF, (*18*)) was performed to check the eventual microheterogeneity of the enzyme. A vertical polyacrylamide Minigel system (Biorad) was utilized. The pH range of the ampholyte was 2.5 to 5 in a 5% (w/v) polyacrylamide gel (prepared from Ready Mix IEF from Pharmacia). Proteins samples were mixed with the same volume of 60% glycerol and 4% Pharmalyte (Pharmacia). Focusing was performed at 200 V for 1 hour, and then at 300 V for two additional hours. The resulting gel was rinsed and the pH gradient was measured with a flat bottom pH electrode (Metrohm). The gel was then stained with 0.1% Coomassie Blue R-250 in 10% methanol and 0.5% acetic acid for 10 min. Background destaining was performed by quick rinsing in 10% methanol. Laccase activity of the different isoenzymes was assayed by incubating the gel in 50 mM citrate/phosphate buffer (CPB) pH 5 containing 1% guaiacol (v/v). Enzymatically active protein bands appeared brown.

Crystallization, Data Collection, and Processing. All steps have been described elsewhere (*11*). Briefly, crystals were grown at 20 °C in a sodium cacodylate buffer pH 6.5, using poly(ethylene glycol) 8000 and zinc acetate as precipitants. A bundle of blue crystals appeared after a few days. Data were collected at 100 K on a rotating anode generator, using glycerol as a cryoprotectant, and processed up to 2.4 Å resolution. Crystals belong to the monoclinic space group $P2_1$, with unit-cell dimensions $a = 87.7$, $b = 110.5$, $c =$

[1] Abbreviations: ABTS: 2,2′-azino-bis(3-ethylbenzthiazoline-6-sulfonic acid); CPB: citrate/phosphate buffer; EPR: electron paramagnetic resonance; 2HF: *N*′,*N*′-dimethyl-*N*-(2-hydroxyphenyl)urea; 2HF-4Cl: *N*′,*N*′-dimethyl-*N*-(4-chloro-2-hydroxyphenyl)urea; 2HF-5Cl: *N*′,*N*′-dimethyl-*N*-(5-chloro-2-hydroxyphenyl)urea; 4HF: *N*′,*N*′-dimethyl-*N*-(4-hydroxyphenyl)urea; 4HF-5Cl: *N*′,*N*′-dimethyl-*N*-(5-chloro-4-hydroxyphenyl)urea; HPLC: high performance liquid chromatography; IEF: isoelectric focusing; Lac-Cc: the *Coprinus cinereus* laccase (pdb accesssion number 1A65); LacIIIb: the *Trametes versicolor* laccase (sequence accession number AF414109); MS: mass spectrometry.

Table 1: Refinement Statistics

resolution range (Å)	35−2.4
R_{cryst}[a] (%)	25.3
R_{free}[b] (%)	27.6
residues	1−499
no. of water molecules	791
r.m.s. deviations	
bond lengths (Å)	0.0075
bond angles (°)	1.47
average B factor (Å^2)	
protein	37.6
Cu (T1, T3)	46.8
Cu (T2)	74.6
2,5-xylidine	50.5
sugars	70.2
water molecules	42.1
Ramachandran statistics[c] (%)	
most favored regions	83.4
additional allowed regions	16.6
overall G factor	0.20

[a] $R_{cryst} = \Sigma\ ||F_{obs}| - |F_{calc}||/\Sigma\ |F_{obs}|$, where $|F_{obs}|$ and $|F_{calc}|$ are the observed and calculated structure factor amplitudes, respectively. [b] R_{free} is the same as R_{cryst} but calculated with a 5% subset of all reflections that was never used in crystallographic refinement. [c] As evaluated by PROCHECK (*35*).

123.2 Å, $\beta = 103.4°$. The unit cell contains four molecules per asymmetric unit.

Phasing, Model Building, and Structure Refinement. The structure was solved by molecular replacement with AMoRe (*19*) in the resolution range 15.0−3.5 Å, using the laccase from *Coprinus cinereus* (pdb code 1A65) as the search model. This enzyme shares 57.7% sequence identity with LacIIIb. The model included the entire polypeptide, without copper atoms or *O*-linked sugars. After rigid-body refinement, the correlation coefficient was 41.4%, and the initial R factor 45.7%.

Models were built using O (*20*). CNS (*21*) version 1.1 was used for refinement, using a maximum-likelihood strategy. After a few cycles of refinement, the initial electron density maps unambiguously revealed the presence of the four coppers in all molecules of the asymmetric unit. Clear density present in the active site was attributed to 2,5-xylidine. Bulk solvent correction and simulating annealing were used, as well as constraints corresponding to noncrystallographic symmetry (NCS). NCS was not applied to coppers, sugars, and 2,5-xylidine. In the final steps, the model was refined using individual B factors. Water molecules were placed in residual density above 2.5 standard deviations, using the "*hbond*" parameters of CNS. Side chains from a few residues had no clear density and were modeled as alanines. Details of the final model quality are given in Table 1.

Enzyme Activity Assays. Laccase activity was determined at 30 °C by oxidation of ABTS into a stable cationic radical ABTS$^{\bullet+}$ (*22*) assayed at 420 nm. Ten microliters of the enzyme solution were added to 990 μL of 0.1 M CPB at pH 3 containing 1 mM ABTS and aerated by bubbling with air prior to the experiment to ensure oxygen saturation. In such conditions, an enzyme solution of one unit/mL was required to oxidize one micromole of ABTS per minute.

Synthesis of Hydroxyphenylurea Compounds. *N*′,*N*′-dimethyl-*N*-(2-hydroxyphenyl)urea (2HF) and *N*′,*N*′-dimethyl-*N*-(5-chloro-2-hydroxyphenyl)urea (2HF-5Cl) were prepared according to previously reported procedures (*23*), which describe the formation of 2-hydroxyphenylureas using a reaction between benzoxazolone (or corresponding 5-chloro substituted compounds) and alkylamines. *N*′,*N*′-dimethyl-*N*-(4-chloro-2-hydroxyphenyl)urea (2HF-4Cl), *N*′,*N*′-dimethyl-*N*-(4-hydroxyphenyl)urea (4HF), and *N*′,*N*′-dimethyl-*N*-(5-chloro-4-hydroxyphenyl)urea (4HF-5Cl) were prepared according to a five-step procedure starting from a methyl-hydroxybenzoate (*23*). This method was slightly adapted for the synthesis of the chlorinated compounds: the two last steps were replaced by a concomitant aminolysis reaction of both acetyl and isocyanate groups of the acetylchlorophenylisocyanates. This was achieved in an excess of liquid dimethylamine in either dry toluene or dichloromethane.

Table 2: Kinetic Parameters of the Purified LacIIIb with Different Substrates

	K_m (mM)		k_{cat} (s^{-1})	
substrate	pH 3	pH 5	pH 3	pH 5
ABTS	0.060	0.085	220	64
2HF	1.8	0.23	38	32
2HF-4Cl	1.6	0.38	290	140
2HF-5Cl	1.2	0.24	87	63
4HF	4.4	0.60	72	47
4HF-5Cl	0.74	0.22	82	97

The structure of the compounds described here, and that of their precursors, were confirmed by ^{1}H- and ^{13}C-nuclear magnetic resonance spectroscopy, mass spectrometry, and infrared spectroscopy.

High Performance Liquid Chromatography. HPLC analyses employed a Varian system including a 9010 pump and a UV−Vis 9050 detector. Twenty microliter samples were analyzed using a reverse-phase Nova Pack C8 column (Waters). The flow rate throughout the analysis was 1 mL min^{-1}. UV absorbency of the eluent was measured at 254 nm. Several water/acetonitrile gradients were used:

Method I: hydroxyphenylurea derivatives were eluted by the following gradient: 0 to 3 min 100:0; 3 to 13 min ramped to 70:30; 13 to 14 ramped to 0:100; 14 to 20 held to 0:100.

Method II: the gradient for 2,5-xylidine analysis was 0 to 15 min, 50:50; 15 to 17 min ramped to 0:100; 17 to 27 min, held at 0:100; 27 to 30 min, ramped to 50:50.

Determination of Kinetic Parameters of ABTS and Hydroxyphenylurea Derivatives. Experiments were performed at 30 °C in aerated 50 mM CPB at pH 3 and 5. Laccase concentrations, measured at 280 nm, ranged from 10^{-9} to 10^{-8} M in the assays, whereas substrate concentrations were in the range 0.01−2 mM. Time course of ABTS oxidation was followed for 2 min at 420 nm. Hydroxyphenylureas were incubated around 30 min in the presence of laccase, and successive aliquots (0.9 mL) were removed. The substrate transformation was stopped by lowering the pH to 1−2 with 0.1 mL of 10% trichloroacetic acid. Kinetic parameters were then determined using HPLC analysis (method I) to separate substrate and product compounds. In the range of substrate concentration used, the initial rate of hydroxylated phenylureas oxidation by laccase was consistent with the Michaelis−Menten equation. The parameters obtained are listed in Table 2.

Transformation of 2,5-Xylidine by LacIIIb. 2,5-Xylidine (0.8 mM in 50 mM CPB pH 5, aerated prior to the experiment) was incubated with 0.25 U/mL of laccase at 30 °C in darkness. A negative control without laccase was

FIGURE 1: The global fold of LacIIIb. Ribbon representation showing the secondary structures. Domain 1 is colored orange, domain 2 is magenta, and domain 3 is dark blue. Copper atoms are indicated as cyan spheres, and labeled: 1 for the "blue" copper of the T1 site, 2 for the depletable copper of the T2 site, 3a and 3b for the coupled coppers of the T3 site. The four glycosylation sites are indicated by circles (full when sites are apparent in the orientation of the figure, empty when they are hindered). 2,5-Xylidine is indicated in ball-and-stick with green sticks (carbon atoms are dark gray, and the nitrogen atom is blue). Drawn with Molscript (*36*) and Raster3D (*37*).

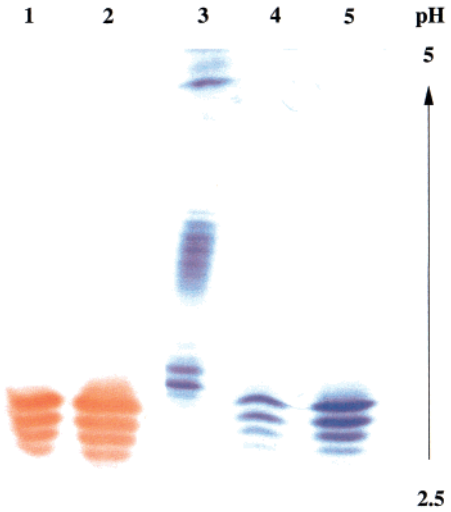

FIGURE 2: Isoelectric focusing of the purified laccase. Purified laccase samples (100 μg per lane) were analyzed in the pH range from 2.5 to 5. Lane 3 contains 20 μg of Sigma IEF standard protein mix. The two first lanes were stained with guaiacol to reveal laccase activity. Lanes 3−5 were stained for proteins with Coomassie R-250 blue. Lanes 1 and 4 show a laccase sample after the first purification step on a DEAE 52 column. In lanes 2 and 5, the sample was further chromatographed on a Phenyl Sepharose column.

performed in parallel. Successive 1-mL aliquots were removed, filtered (Millipore 0.45 μM), and analyzed by HPLC according to method II.

RESULTS

The Global Fold of the Crystal Structure. The structure is globular with approximate dimensions of 70 × 50 × 50 Å. It consists mainly of antiparallel β-barrels (Figure 1). There are three cupredoxin-like domains: the T1 site (Cu1) belongs to domain 3 (dark blue on Figure 1), and the T2/T3 site (Cu2, Cu3a, and Cu3b) is at the interface between the two other domains (orange and magenta, upper part of Figure 1). This topology is essentially the same as that from the monomer of Zucchini ascorbate oxidase (*16*). The overall structure is very close to that of the Cu2-depleted form of Lac-Cc (*13*). The electron density indicates glycosylation sites of LacIIIb and allows unambiguous determination of both the T1 and the trinuclear T2/T3 copper sites. As was described for ascorbate oxidase and Lac-Cc, there is a putative binding cavity for reducing substrates in the vicinity of Cu1. Clear electron density is present in this cavity, consistent with bound 2,5-xylidine.

The Four N-Glycosylation Sites Observed in the Crystal Structure. IEF experiments on the purified *T. versicolor* enzyme (Figure 2) indicates five different isozymes. Their isoelectric points are rather close: 3.23 (for isozyme 1), 3.11 (isozyme 2), 3.0 (isozyme 3), 2.88 (isozyme 4), and 2.75 (isozyme 5). These laccase isozymes probably differ by their glycosylation. LacIIIb was expressed in fungus cultures, and not overexpressed in a different species (bacterium or yeast), and the purified enzyme was not deglycosylated before crystallization. This gave an opportunity to study its natural posttranslational modifications. There are six putative *N*-glycosylation sites (consensus sequence Asn-X-Thr): asparagines 51, 54, 208, 217, 333, and 436. The density maps clearly indicate glycosylation on asparagines 54, 217, 333, and 436. In all cases, the first *N*-acetyl-glucosamine could be modeled in the density. The glycosylation could be extended up to four supplementary osidic residues, depending on the site, and for a particular site on the molecule of the asymmetric unit.

The glycosylation observed in the crystal structure of LacIIIb is consistent with mass spectrometry experiments. Isozymes 1 and 2 of LacIIIb, the most abundant forms, were separated by cutting IEF bands, and proteolyzed by trypsin. The resulting fragments were attributed on the basis of their molecular weights in MALDI-TOF mass spectrometry (not shown). Fragments that could not be attributed suggested a posttranslational modification. For instance, the glycosylation of Asn 436 explains why the expected 424−440 fragment remains absent in mass spectrometry experiments for isozyme 1. In contrast, this fragment is found with the isozyme 2. This suggests that the crystallized enzyme, glycosylated on Asn 436, corresponds to the isozyme 1, the most abundant one.

*The trinuclear T2/*T3 copper site. The trinuclear center is coordinated to eight histidines (Figure 3a). Six of them coordinate Cu3a and Cu3b: histidines 66, 109, and 454 for Cu3a, and histidines 111, 400, and 452 for Cu3b. In addition, the bridging oxygen atom from the hydroxide known to bind both Cu3a and Cu3b is equidistant from these two coppers. The oxygen−Cu3a distance is 1.8−1.9 Å, depending on the molecule of the asymmetric unit, and the oxygen−Cu3b distance is 1.8−2.0 Å. This results in a Cu3a−Cu3b distance of 3.75 Å.

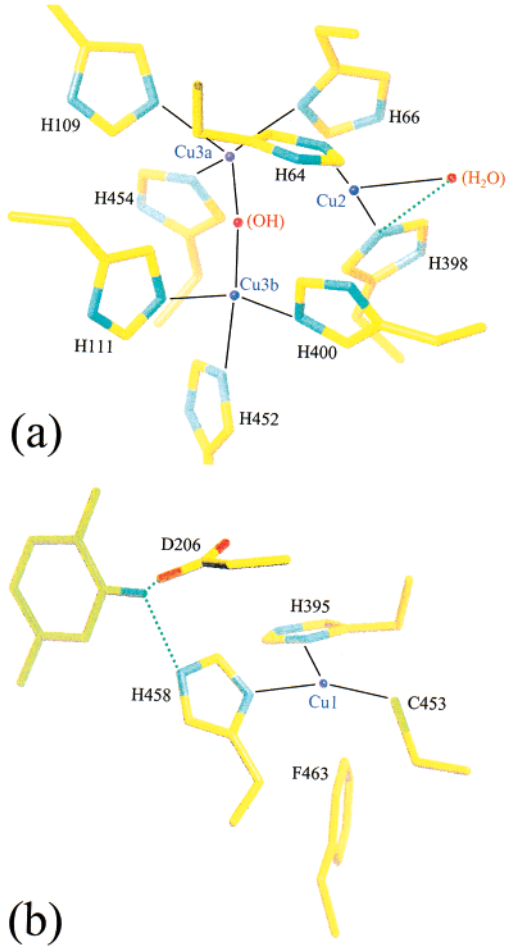

FIGURE 3: The copper sites of LacIIIb and their environment. (a) The trinuclear T2/T3 site. Histidine side chains involved in copper binding (copper atoms are blue) are in sticks (C atoms are yellow, N atoms are cyan), and labeled. Oxygen atoms involved in copper cordination are red. Copper coordinations are indicated with dark lines. Dotted lines indicate interacting atoms distant from less than 3.2 Å. Drawn with Turbo (*38*). (b) The T1 site and the neighboring 2,5-xylidine ligand. The side chains of the copper-coordinating histidines and cysteine are drawn. Also indicated are the side chains of the noncoordinating Phe 463, and of the Asp 206 residue that interacts with 2,5-xylidine (green model).

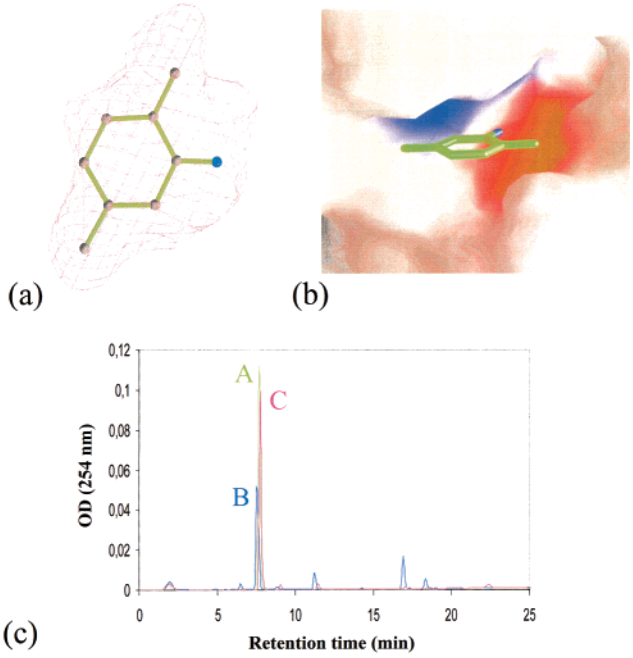

FIGURE 4: The 2,5-xylidine present in the putative reducing substrate cavity is a laccase substrate. (a) Electron density of the 2,5-xylidine ligand. F_o-F_c omit map (magenta) calculated in the absence of the ligand. The contour level is at 3 standard deviations of the map. The refined model of 2,5-xylidine is shown. The figure was prepared with Bobscript (*39*) and Raster3D. (b) The molecular surface of the binding pocket that encloses 2,5-xylidine. Viewed from the entrance of the cavity (corresponding to the left side in the orientation of Figure 1). The red negative zone corresponds to the side chain of Asp 206. The blue positive zone, partly hidden by the upper edge of the cavity, corresponds to the side chain of His 458. Drawn with GRASP (*40*). (c) Transformation of 2,5-xylidine by laccase at pH 5. HPLC analysis (method II). Peak A corresponds to 2,5-xylidine at the beginning of experiment. Peak B is observed after 20 h incubation with laccase. Peak C is the negative control (without enzyme) after 20 h incubation.

Cu2 is coordinated to histidines 64 and 398, and to a water molecule from the solvent. The Cu2−water distance varies notably among the four different molecules of an asymmetric unit (2.3−2.9 Å).

The Culture Inducer 2,5-Xylidine Is Present in the Cavity Close to Cu1. The electron density indicates the presence of a ligand molecule in the putative cavity for the reducing substrate. Figure 4a shows that the omit map is in good accordance with the model of 2,5-xylidine. This arylamine was initially used in the fungus culture medium for laccase induction. Figure 4b shows a model of the ligand enclosed in its binding cavity.

Given its presence at the active site, we checked whether 2,5-xylidine could be a laccase substrate (Figure 4c). After 20 h of incubation in the presence of laccase (pH 5, 30 °C), 38% of the 2,5-xylidine was transformed, and significant new peaks appeared. The products corresponding to these new peaks had higher retention times, indicating that they were more hydrophobic than the arylamine substrate.

The T1 Copper Site and the Neighboring Cavity that Binds 2,5-Xylidine. Cu1 is coordinated to histidines 395 and 458, and to Cys 453 (Figure 3b). The noncoordinated Phe 463 residue is at a distance of 3.7 Å from the copper. This phenylalanine is homologous to the axial methionine coordinated to the copper of the T1 site in ascorbate oxidase. In LacIIIb structure, the histidine ring of His 458 (which is coordinated to Cu1) is close to the nitrogen from 2,5-xylidine: distances between enzyme and substrate nitrogens are less than 3.2 Å, consistent with a hydrogen bond, for all molecules of an asymmetric unit, except in molecule C. In this latter case, the distance is 4 Å.

The amino group of 2,5-xylidine is also hydrogen bonded to a terminal oxygen of Asp 206 side chain. In addition, for molecule C (in which His 458 is not hydrogen bonded to the arylamine) the second terminal oxygen is also hydrogen bonded to 2,5-xylidine, making a bidentate interaction. Besides these hydrogen bonds, there are many hydrophobic protein−ligand interactions (Figure 5, dark blue). They involve Phe 162, Leu 164, and Phe 265 residues, all belonging to two neighboring loops (above 2,5-xylidine in the orientation of Figure 5a) which delineate the cavity. On the opposite side (below the ligand on Figure 5a), two hydrophobic residues (phenylalanines 332 and 337) constitute the other wall of the cavity. This cavity is rather wide (approximate dimensions 10 × 10 × 20 Å), so that the observed ligand is not tightly buried in it (Figure 4b).

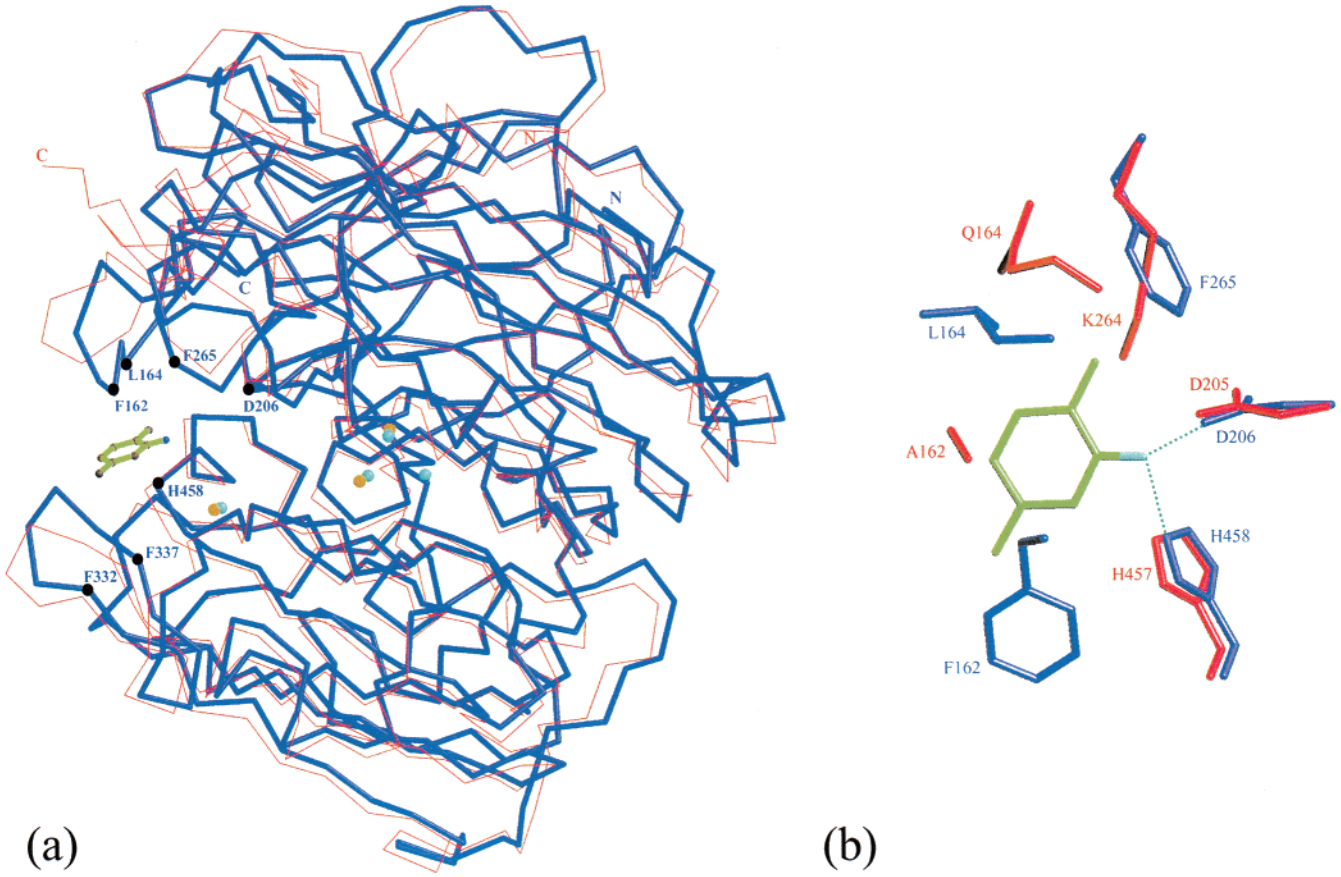

FIGURE 5: Superposition of the laccases from *Trametes versicolor* (LacIIIb) and from *Coprinus cinereus* (Lac-Cc). (a) Overall view. The LacIIIb backbone is represented as a thick dark blue trace, and that of Lac-Cc as a thin red trace. Coppers are cyan for Lac-Cc, and yellow for LacIIIb. The positions of the residues interacting with 2,5-xylidine are marked with full circles, and labeled. Drawn with Molscript and Raster3D. (b) Magnification of the 2,5-xylidine and neighboring interacting residues of the reducing substrate cavity. Side chains of LacIIIb residues are dark blue. Corresponding residues of Lac-Cc are red. Drawn with Turbo.

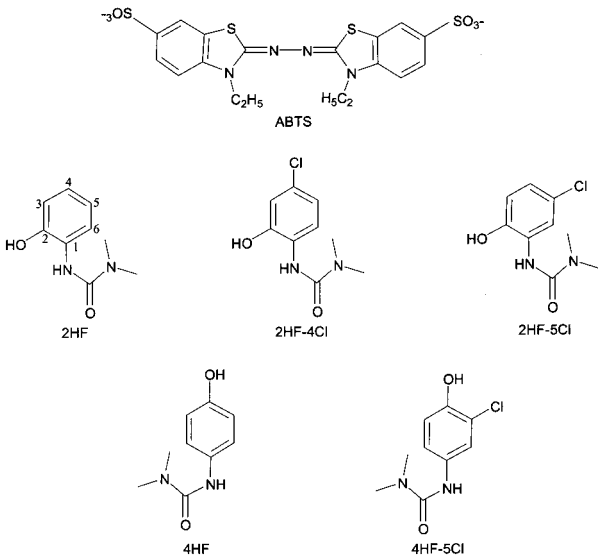

FIGURE 6: Schematic representation of LacIIIb substrates assayed for kinetic parameters determination. Drawn with ChemDraw.

Activity of the Purified Enzyme. Laccase-catalyzed oxidation of hydroxyphenylurea derivatives and of the nonphenolic model substrate ABTS (shown on Figure 6) was examined at pH 3 and 5. All kinetic parameters of hydroxyphenylureas are in the same order of magnitude: K_m values range from 0.22 to 4.4 mM, and k_{cat} from 32 to 290 s^{-1} (Table 2). The highest oxidation rate (based on k_{cat}/K_m values) was for 4HF-5Cl at pH 5, the lowest for 2HF and 4HF at pH 3. Increasing the pH from 3 to 5 induces a significant increase in the affinity for each of the hydroxyphenylurea derivatives. As phenols are natural substrates for laccase, it can be supposed that the nature and position of substituents on the phenolic ring is a key element of substrate docking in the active center. Among the hydroxyphenylureas studied, the derivative with a *para*-hydroxyl substituent, 4HF, shows the lowest affinity (specially at pH 3, with a K_m value of 4.4 mM), although this substitution position is expected to induce the weakest steric hindrance, as referred to the phenolic group. Actually, both at pH 3 and 5, the derivatives with an *ortho* substituent (as referred to the hydroxyl) have relatively good affinities, whatever the substituent is an urea (2HF has a lower K_m than 4HF) or a chlorine (4HF-5Cl has a lower K_m than 4HF). Such a result was also observed by Xu (*24*): all *ortho*-substituted phenols exhibited a better affinity than phenol itself for the recombinant laccase from *Trametes villosa*. At pH 3, the addition of a chlorinated substituent to the aromatic ring induces a positive effect on the binding affinity of the substrate. The largest effect is observed for 4HF-5Cl versus 4HF.

DISCUSSION

The Trinuclear T2/T3 Copper Site: Why Is Cu2 Labile? In the previously published structure of *C. cinereus* laccase, the extremely high mosaicity of crystals grown from the native enzyme prevented X-ray studies. Therefore, to get

crystals suitable for data collection, enzymatic deglycosylation was necessary, but it caused the loss of Cu2 (*25*). On the other hand, with *T. versicolor* laccase a complete data set could be collected at 2.4 Å with the native enzyme, despite a high mosaicity of the crystals (1.3°, as refined by SCALEPACK (*26*)). This allows for the first time a complete description of the trinuclear copper center.

The distance between the two coppers of the T3 site is 3.75 Å. This is close to values observed for other multicopper oxidases of known three-dimensional structure (around 3.7 Å for both ascorbate oxidase (*16*) and ceruloplasmin (*27*)). However, in the structure of Lac-Cc, the hydroxide bridging Cu3a no longer bridged Cu3b, and the Cu3a−Cu3b distance was larger (around 5 Å, (*13*, *14*)). As was suggested by the authors, this longer distance probably reflects the absence of Cu2. Beside Cu2 depletion, modifications of the enzyme oxidation state can also increase the Cu3a−Cu3b distance and alter the binding of the oxygen bridging the Cu3 atoms. For instance, in the case of ascorbate oxidase the Cu3a−Cu3b distance increases from 3.74 Å for the natural, oxidized form (*16*) to values ranging from 4.8 to 5.1 Å for the reduced, peroxide, and azide forms of the enzyme, where no oxygen bridges Cu3a and Cu3b (*28*).

In *T. versicolor* laccase, either Cu3a or Cu3b is bound to three histidines and an oxygen atom, while Cu2 is coordinated to only two histidines, and to a water molecule. The same feature was found for the trinuclear copper site of ascorbate oxidase (pdb code 1AOZ) in which Cu2 is depletable (although the crystal structure of T2-depleted ascorbate oxidase indicates that the copper, mostly lost from the T2 site, is also lost from the T3 site (*29*)). Moreover, in LacIIIb structure the position of the coordinated water molecule significantly varies among the four different molecules of the asymmetric unit, indicating that Cu2 is only weakly coordinated to this water. This gives a structural basis to the lability of Cu2.

Circular dichroism and low-temperature magnetic circular dichroism have been performed on a type 1 Hg^{2+}-substituted derivative (T1 copper substituted with Hg^{2+}) of the plant laccase from *Rhus vernicifera*. The assigned ligand field transition energies indicate that all three copper ions from the T2/T3 center have tetragonal geometries (*30*). This led to the hypothesis that an oxygen ligand was present in the center of the trinuclear copper site (*31*). However, in the structure of the T2/T3 site of LacIIIb both T3 coppers are tetrahedrally coordinated, and the T2 copper has three ligands. No density attributable to an oxygen atom can be seen in the center of the trinuclear copper site. Thus, this T2/T3 site is essentially the same as that of ascorbate oxidase (*16*). Therefore, our results protract the observed discrepancy between the interpretation of spectroscopy of *R. vernicifera* laccase and the crystal structures of multicopper oxidases.

The Presence of 2,5-Xylidine Bound to the Crystallized Enzyme. An electron density consistent with 2,5-xylidine was found in the cavity close to the T1 copper site, indicating the presence of this arylamine in the crystals. Most inducers of fungal laccases are substrates of the enzyme to be produced, or substances structurally similar to these substrates. 2,5-Xylidine, a usual laccase inducer (*32*), was used in the culture medium for *T. versicolor*. Incubation of 2,5-xylidine with the purified enzyme showed that this arylamine is a substrate, although very poor: comparative experiments were performed at pH 5 and 30 °C with a same amount of laccase (0.25 U/mL) and of the different substrates (0.8 mM). In such conditions, no significant transformation of 2,5-xylidine (less than 5%) occurs after 4 h, whereas both 2HF-5Cl and ABTS are completely transformed in less than 10 minutes. It must also be kept in mind that the conditions chosen to test laccase-catalyzed oxidation of 2,5-xylidine were the most favorable. In contrast, in the mother liquor used for crystallization, the controlled temperature was 20 °C. Moreover, the pH was 6.5, a value for which LacIIIb is almost inactive with hydroxyphenylurea substrates (not shown). Thus, the transformation of 2,5-xylidine should be very slow in the crystallization drop. Otherwise, the crystallization process could have selected a small subpopulation of the enzyme that bound 2,5-xylidine. In this case, the substrate would only be present at a low level in the purified enzyme preparation.

In the small electron-transporting cupredoxins, a main chain carbonyl oxygen coordinates the axial position of Cu1. An equivalent carbonyl is also present in multicopper oxidases, but is displaced away from the T1 site by a main chain rearrangement, resulting in the formation of a putative binding cavity for the reducing substrate (*13*). The structure of LacIIIb complexed to 2,5-xylidine is the first high-resolution structure with an organic reducing substrate in this cavity, close to Cu1.

Contribution to Electron-Transfer Analysis. The catalytic activity of laccases implies an electron transfer from Cu1 to the trinuclear T2/T3 site. This transfer may be through-bond, through-space, or a combination of both. The LacIIIb structure provides two branched through-bond pathways starting from Cu1, both involving Cys 453 and a contiguous histidine. The first one leads to Cu3a through His 454, and the second one to Cu3b through His 452 (see Figure 3). In the alternate through-space theory, it has been calculated that electron tunneling in proteins between redox centers that are distant of 14 Å or less does not imply the need for an optimal route through residues selected by the evolution (*33*). In *T. versicolor* laccase, the distance between Cu1 and Cu3a is 12.8 Å, that between Cu1 and Cu3b is 12.2 Å. Therefore, the structure is also consistent with a through-space transfer.

Concerning the electron-transfer associated with the reduction of Cu1 by the substrate, the structure presented here gives information (Figure 3b). The proximity of His 458, which coordinates Cu1, with the amino group of 2,5-xylidine, from which an electron is extracted by the enzyme, suggests that His 458 is the entrance door of this electron during its transfer to Cu1. This could explain the importance of site-directed mutagenesis of the contiguous sequence LEA (Leu 459−Glu 460−Ala 461 in LacIIIb) for the catalytic activity and pH dependence of fungal laccases (*34*). The Cu1-coordinating His 458 is highly conserved in all multicopper oxidases.

The Cavity for the Reducing Substrate: Possibility of a Ligand-Induced Closure. The backbones of *T. versicolor* and *C. cinereus* laccases are extremely similar, except for the longer C-terminal region of Lac-Cc (Figure 5a). The only significant difference involves the external loops surrounding the 2,5-xylidine binding site: the cavity is more closed in the case of LacIIIb. There are three possible explanations: (i) an artifactual difference due to the different crystal packings of LacIIIb and Lac-Cc, possibly induced by the

different glycosylation levels; (ii) a species variation related to the sequence difference between *T. versicolor* and *C. cinereus* laccases; (iii) an induced-fit closing movement of LacIIIb due to the presence of a bound ligand. At present, we have no way to suggest which explanation is the right one.

The cavity for the reducing substrate appears far more surrounded by hydrophobic side chains in LacIIIb than in Lac-Cc. The hydrophobic residues Leu 164 and Phe 265 of *T. versicolor* laccase (above 2,5-xylidine in the orientation of Figure 5a) replace the corresponding polar (Gln 164) and charged (Lys 264) residues of *C. cinereus* enzyme. These two residues belong to loops that are closer in LacIIIb structure than in that of Lac-Cc. Moreover, the hydrophobic residue Phe 162 of LacIIIb is larger, and closer from the 2,5-xylidine position, than the corresponding Ala 162 from *C. cinereus* enzyme (Figure 5b). The opposite side of the ligand (below it on Figure 5a) also shows a loop that is closer for LacIIIb. This loop contains the phenylalanines 332 and 337, which make hydrophobic interactions with the ligand, and are conserved in both enzymes. To summarize, the loops of *T. versicolor* laccase that appear more closed upon the substrate cavity contain 2,5-xylidine interacting residues. This is consistent with a possible ligand-induced fit of laccases.

Correlation of the Structure with the pH Dependence of Hydroxyphenylureas Affinities. For all five synthesized hydroxyphenylurea compounds, the affinities reflected by K_m values are significantly better at pH 5 than at pH 3 (Table 2). No chemical deprotonation of the phenolic group of these substrates is expected in the 3−5 pH range. Thus, the observed effect of pH can be related to pK_a values of laccase side chains interacting with the oxidized substrate substituent: an amino substituent for 2,5-xylidine and other arylamines, an hydroxyl substituent for phenolic substrates. The structure indicates that the amino substituent of 2,5-xylidine is hydrogen bonded to Asp 206 in all four molecules of the asymmetric unit. The typical pK_a value for an aspartate side chain is 3.9, allowing different protonation states for pH 3 and pH 5. At pH 5, the carboxylic function of Asp 206 is dissociated, so that its negative charge should stabilize the partial positive charge of the hydrogen extracted from the reducing substrate by the enzyme. Conversely, at pH 3 the side chain of Asp 206 is not dissociated, which is less favorable for the reduction process.

With ABTS there is no significant difference in K_m values between pH 3 and pH 5. ABTS differs from phenolic substrates because its oxidation does not involve proton transfer, but only a single electron transfer. Thus, as with ABTS no hydrogen can be extracted from the reducing substrate, the pH-dependent stabilizing role of Asp 206 is not observed. This is consistent with the proposed essential role of this residue in the laccase-catalyzed oxidation of arylamine or phenol substrates. Asp 206 is well conserved among fungal laccases. It is also contiguous to Cys 205, a residue involved in a disulfide bond conserved in fungal laccases.

ACKNOWLEDGMENT

We thank Joël Janin (CNRS UPR 9063) for helpful discussion about the manuscript.

REFERENCES

1. Solomon, E. I., Sundaram, U. M., and Machonkin, T. E. (1996) *Chem. Rev. 96*, 2536−2605.
2. McGuirl, M. A., and Dooley, D. (1999) *Curr. Opin. Chem. Biol. 3*, 138−144.
3. Gianfreda, L., Xu, F., and Bollag, J. M. (1999) *Biorem. J. 3*, 1−25.
4. Briggs, G. G., and Ogilvie, S. Y. (1971) *Pestic. Sci. 2*, 165−168.
5. Roberts, T. R., Hutson, D. H., Lee, P. W., Nicholls, P. H., and Plimmer, J. R. (1998) *Metabolic Pathways of Agrochemicals*, The Royal Society of Chemistry, Cambridge, UK.
6. Frear, D. S., and Swanson, H. R. (1974) *Phytochemistry 13*, 357−360.
7. Tanaka, F. S., Wien, R. G., and Zaylskie, R. G. (1977) *J. Agric. Food Chem. 25*, 1068−1072.
8. Aguer, J. P., and Richard, C. (1996) *Pestic. Sci. 46*, 151−155.
9. Cameron, M. D., Timofeevski, S., and Aust, S. D. (2000) *Appl. Microbiol. Biotechnol. 54*, 751−758.
10. Ullah, M. A., Bedford, C. T., and Evans, C. S. (2000) *Appl. Microbiol. Biotechnol. 53*, 230−234.
11. Bertrand, T., Jolivalt, C., Caminade, E., Joly, N., Mougin, C., and Briozzo, P. (2002) *Acta Crystallog. Sect. D 58*, 319−321.
12. Mikuni, J., and Morohoshi, N. (1997) *FEMS Microbiol. Lett. 155*, 79−84.
13. Ducros, V., Brzozowski, A. M., Wilson, K. S., Brown, S. H., Ostergaard, P., Schneider, P., Yaver, D. S., Pedersen, A. H., and Davies, G. J. (1998) *Nat. Struct. Biol. 5*, 310−316.
14. Ducros, V., Brzozowski, A. M., Wilson, K. S., Ostergaard, P., Schneider, P., Svendson, A., and Davies, G. J. (2001) *Acta Crystallog. Sect. D 57*, 333−336.
15. Reinhammar, B., and Oda, Y. (1979) *J. Inorg. Biochem. 11*, 115−27.
16. Messerschmidt, A., Ladenstein, R., Huber, R., Bolognesi, M., Avigliano, L., Petruzzelli, R., Rossi, A., and Finazzi-Agro, A. (1992) *J. Mol. Biol. 224*, 179−205.
17. Zaitsev, V. N., Zaitseva, I., Papiz, M., and Lindley, P. F. (1999) *J. Biol. Inorg. Chem. 4*, 579−587.
18. Robertson, E. F., Dannelly, H. K., Malloiy, P. J., and Reeves, H. C. (1987) *Anal. Biochem. 167*, 290−294.
19. Navaza, J. (1994) *Acta Crystallog. Sect. A 50*, 157−163.
20. Jones, T. A., Zou, J. Y., Cowan, S. W., and Kjeldgaard, M. (1991) *Acta Crystallog. Sect. A 47*, 110−119.
21. Brünger, A. T., Adams, P. D., Clore, G. M., DeLano, W. L., Gros, P., and Grosse-Kunstleve, R. W. et al. (1998) *Acta Crystallog. Sect. D 54*, 905−921.
22. Wolfenden, B. S., and Wilson, R. L. (1982) *J. Chem. Soc., Perkin Trans. 2*, 805−812.
23. Jolivalt, C., Raynal, A., Caminade, E., Kokel, B., Le Goffic, F., and Mougin, C. (1999) *Appl. Microbiol. Biotechnol. 51*, 676−681.
24. Xu, F. (1996) *Biochemistry 35*, 7608−7614.
25. Ducros, V., Davies, G. J., Lawson, D. M., Wilson, K. S., Brown, S. H., Ostergaard, P., Pedersen, A. H., Schneider, P., Yaver, D. S., and Brzozowski, A. M. (1997) *Acta Crystallog. Sect. D 53*, 605−607.
26. Otwinowski, Z., and Minor, W. (1993) DENZO, a film processing program for macromolecular crystallography, New Haven, CT.
27. Zaitseva, I., Zaitsev, V., Card, G., Moshkov, K., Bax, B., Ralph, A., and Lindley, P. F. (1996) *J. Biol. Inorg. Chem. 1*, 15−23.
28. Messerschmidt, A., Luecke, H., and Huber, R. (1993) *J. Mol. Biol. 230*, 997−1014.
29. Messerschmidt, A., Steigemann, W., Huber, R., Lang, G., and Kroneck, P. M. (1992) *Eur. J. Biochem. 209*, 597−602.
30. Solomon, E. I., Lowery, M. D., LaCroix, L., and Root, D. E. (1993) *Methods Enzymol. 226*, 1−33.
31. Cole, J. L., Clark, P. A., and Solomon, E. I. (1990) *J. Am. Chem. Soc. 112*, 9534−9548.
32. Fahraeus, G., Tullander, V., and Ljunggren, H. (1958) *Physiol. Plant. 11*, 631−643.

33. Page, C. C., Moser, C. C., Chen, X., and Dutton, L. (1999) *Nature 402*, 47−52.
34. Xu, F., Berka, R. M., Wahleithner, J. A., Nelson, B. A., Shuster, J. R., Brown, S. H., Palmer, A. E., and Solomon, E. I. (1998) *Biochem. J. 334*, 63−70.
35. Laskowski, R. A., MacArthur, M. W., Moss, D. S., and Thornton, J. M. (1993) *J. Appl. Crystallogr. 24*, 946−950.
36. Kraulis, P. (1991) *J. Appl. Crystallogr. 24*, 946−950.
37. Merritt, E. A., and Bacon, D. (1997) *Methods Enzymol. 277*, 505−524.
38. Roussel, A., and Cambillau, C. (1989) *Silicon Graphics Geometry Partners Directory*, 77−78.
39. Esnouf, R. M. (1997) *J. Mol. Graphics Modell. 15*, 132−134.
40. Nichols, A., Sharp, K. A., and Honig, B. (1991) *Proteins 11*, 281−296.

BI0201318